

1-1-1975

# Properties of Intercalated 2H-NbSe<sub>2</sub>, 4Hb-TaS<sub>2</sub> and 1T-TaS<sub>2</sub>

S. F. Meyer  
*Stanford University*

R. E. Howard  
*Stanford University*

G. R. Stewart  
*Stanford University*

Juana Vivó Acrivos  
*San Jose State University*, [juana.acrivos@sjsu.edu](mailto:juana.acrivos@sjsu.edu)

T. H. Geballe  
*Stanford University*

Follow this and additional works at: [https://scholarworks.sjsu.edu/chem\\_pub](https://scholarworks.sjsu.edu/chem_pub)

 Part of the [Physical Chemistry Commons](#)

## Recommended Citation

S. F. Meyer, R. E. Howard, G. R. Stewart, Juana Vivó Acrivos, and T. H. Geballe. "Properties of Intercalated 2H-NbSe<sub>2</sub>, 4Hb-TaS<sub>2</sub> and 1T-TaS<sub>2</sub>" *Journal of Chemical Physics* (1975): 4411-4419. doi:10.1063/1.430342

This Article is brought to you for free and open access by the Chemistry at SJSU ScholarWorks. It has been accepted for inclusion in Faculty Publications, Chemistry by an authorized administrator of SJSU ScholarWorks. For more information, please contact [scholarworks@sjsu.edu](mailto:scholarworks@sjsu.edu).

## Properties of intercalated $2\text{HNbSe}_2$ , $4\text{HbTaS}_2$ , and $1\text{TTaS}_2$

S. F. Meyer, R. E. Howard, G. R. Stewart, J. V. Acrivos, and T. H. Geballe

Citation: *J. Chem. Phys.* **62**, 4411 (1975); doi: 10.1063/1.430342

View online: <http://dx.doi.org/10.1063/1.430342>

View Table of Contents: <http://jcp.aip.org/resource/1/JCPSA6/v62/i11>

Published by the [American Institute of Physics](#).

---

### Additional information on *J. Chem. Phys.*


Journal Homepage: <http://jcp.aip.org/>

Journal Information: [http://jcp.aip.org/about/about\\_the\\_journal](http://jcp.aip.org/about/about_the_journal)

Top downloads: [http://jcp.aip.org/features/most\\_downloaded](http://jcp.aip.org/features/most_downloaded)

Information for Authors: <http://jcp.aip.org/authors>

## ADVERTISEMENT



**Special Topic Section:**  
**PHYSICS OF CANCER**

Why cancer? Why physics? [View Articles Now](#)

# Properties of intercalated 2H-NbSe<sub>2</sub>, 4Hb-TaS<sub>2</sub>, and 1T-TaS<sub>2</sub> \*

S. F. Meyer<sup>†</sup>, R. E. Howard, G. R. Stewart, J. V. Acrivos<sup>‡</sup>, and T. H. Geballe

Department of Applied Physics, Stanford University, Stanford, California 94305  
(Received 16 April 1974)

The layered compounds 2H-NbSe<sub>2</sub>, 4Hb-TaS<sub>2</sub>, and 1T-TaS<sub>2</sub> have been intercalated with organic molecules; and the resulting crystal structure, heat capacity, conductivity, and superconductivity have been studied. The coordination in the disulfide layers was found to be unchanged in the product phase. Resistance minima appear and the superconducting transition temperature is reduced in the NbSe<sub>2</sub> complex. Conversely, superconductivity is induced in the 4Hb-TaS<sub>2</sub> complex. Corresponding evidence of a large change of the density of states, negative for 2H-NbSe<sub>2</sub> and positive for 4Hb-TaS<sub>2</sub>, was also observed upon intercalation. The transport properties of all the intercalation complexes show a pronounced dependence upon the coordination of the transition metal.

## I. INTRODUCTION

The dichalcogenides of niobium and tantalum have been investigated extensively in recent years. They can be prepared in single crystal form rather easily and possess a number of unusual temperature-dependent physical properties.<sup>1</sup> These are likely to be related to the response of the lattice to the two-dimensional-like characteristic of the Fermi surface. This has recently been discovered to lead to the formation of charge-density waves and ultimately superlattices.<sup>2</sup> In addition, the very interesting reaction wherein atoms and molecules (I) are inserted between the disulfide layers of the dichalcogenides has initiated many studies.<sup>3</sup> In the resulting intercalation complex, the conduction electrons are almost constrained to propagate within a single dichalcogenide layer which is only 6 Å thick, yet superconductivity is, in many cases, enhanced. The ability to react correlates roughly with the  $pK_a$  value of I.<sup>4</sup> A charge transfer model has been suggested as the stabilization mechanism,<sup>5</sup> some support for which can be found in x-ray photoelectron spectroscopy<sup>4</sup> and nuclear magnetic resonance experiments.<sup>6</sup>

The purpose of this work is twofold. To date, the most stable complexes of TaS<sub>2</sub> are for the 2H polytype in which the tantalum atom is coordinated by a trigonal prism of sulfur atoms, as shown in Fig. 1. The first objective of this work was to search for ligands which form the most stable complexes with the 2H polytype so that other, less reactive polytypes of TaS<sub>2</sub> could be intercalated. The 2H polytype forms imperfect crystals owing to the fact that these are grown as a 1T polytype which is then converted to the former by a phase transition, with a concomitant volume change. The intercalation complexes of the other polytypes are expected to produce sufficiently perfect crystals, enabling study of the superconductivity and the expected anisotropy of the transport properties for the second objective of this work. Previous efforts in this laboratory have involved mixed anion crystals TaS<sub>1.6</sub>Se<sub>0.4</sub>.<sup>7</sup> These, like the selenides, generally form good crystals, and the ease of intercalation possessed by the sulfide crystals is preserved. The above formulas and those used in the rest of this paper refer to trigonal prismatic coordination in the disulfide layer unless designated otherwise.

In the present investigation, as will be evident, we have succeeded in preparing intercalation complexes of

2H-NbSe<sub>2</sub> which form more perfect crystals than the isostructural 2H-TaS<sub>2</sub>. In addition, we have successfully prepared intercalation complexes of semimetallic 1T-TaS<sub>2</sub> in which the coordination of the sulfur atoms about the tantalum is octahedral, and also of the interesting 4Hb-TaS<sub>2</sub> polymorph, shown in Fig. 1, where successive layers are alternately trigonal prismatic and octahedral TaS<sub>2</sub>.<sup>8</sup> We are thus able to study the effect of forming intercalation complexes upon the metallic and superconducting trigonal layers as well as upon the semiconducting (or semimetallic) octahedral layers.

The paper is organized as follows. In Sec. II the methods of preparation and the methods used to characterize the sample, which are similar to those already in the literature, are briefly stated and discussed. In Sec. III the methods for the measurements of resistivity, superconductivity, and heat capacity which have been made on suitable crystals are presented and discussed. In Sec. IV we discuss the results of the measurements, and in Sec. V draw some experimental conclusions.

## II. SAMPLE PREPARATION AND CHARACTERIZATION

The dichalcogenide crystals were prepared from reacted powders using the iodine vapor transport method, as reported elsewhere.<sup>9</sup> The structures of the principal polymorphs grown, shown in Fig. 1, were verified by x-ray diffraction methods. Neat (reagent grade) chemicals were used for sample preparation. Reagents, such as NH<sub>3</sub>, were stored over sodium as liquids under pressure, and the gas handled in a high vacuum system, as reported elsewhere.<sup>10</sup> The reactants (TX<sub>2</sub> crystals and ligands) were sealed in glass ampoules, and dry helium was added to ensure thermal equilibrium during low temperature measurements. The sealed ampoules were reacted at a sufficiently high temperature for intercalation to occur (defined as  $T_{\text{interc}}$  in Table I), but not necessarily the lowest possible temperature. The course of the reaction could, in many cases, be qualitatively followed visually simply by observing the marked swelling of the crystals. In those cases (NbSe<sub>2</sub>) where the superconducting transition decreased upon intercalation, the transition temperature could be used to monitor the reaction. The superconducting transition was determined with the samples remaining inside the sealed reaction tubes containing an excess of the ligand.

The intercalation complexes prepared and charac-

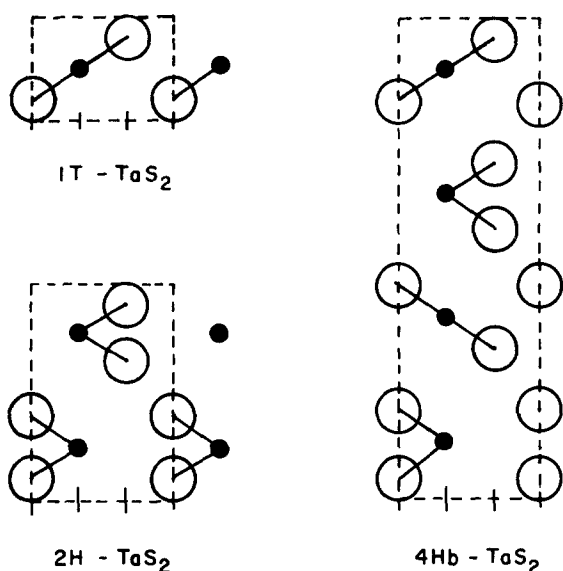


FIG. 1. Crystal structures shown along the  $(11\bar{2})$  plane of three phases of TaS<sub>2</sub>. Note the similarity of the van der Waals gap symmetry in 2H-TaS<sub>2</sub> and 4Hb-TaS<sub>2</sub>.

terized are given in Table I. Ethylenediamine (EDA) was found to react with NbSe<sub>2</sub>, and to form the first known NbSe<sub>2</sub> complexes stable at room temperature.<sup>11</sup> This stability allowed measurements to be made of such properties as heat capacity and resistivity. Ethylenediamine and also triethylamine appear to form stable complexes at room temperature with 4Hb-TaS<sub>2</sub>.

Stoichiometry measurements were difficult for most of the organic ligand complexes. For room temperature gases, such as NH<sub>3</sub>, a manometric method was used. The sample was frozen and placed in a manometer system of known volume. The excess liquid was boiled off under vacuum with the sample maintained at a temperature where the sample was stable. This temperature is noted as  $T_{\text{stable}}$  in Table I and does not imply that it is necessarily the highest stable temperature. When dry, the product was allowed to warm up above  $T_{\text{interc}}$  in order to reverse the intercalation reaction, i.e., "deintercalate." The pressure measurement allowed the calculation of the mole ratio to about 20% accuracy. The accuracy of this measurement was less for methylamine and ethylamine because of adsorption on the sample surface.

In the case of EDA, a standard weight gain method with results accurate to  $\pm 10\%$  was used since the excess reagent could be washed off with isopropanol. Thermogravimetric analysis (TGA) on the EDA complexes showed weight loss at several successive stages, starting at about 50 °C and finishing at 400 °C. The calculated stoichiometry from the total weight loss exceeded the weight gain during intercalation. This excess weight loss indicates that there exists a large binding energy leading to a destructive deintercalation. This might also be due to the rather high temperatures involved in the TGA.

The crystal structure parameters were obtained using a low temperature x-ray mount and a low temperature sample preparation technique. The x-ray slides were

prepared in a nitrogen atmosphere on a working table held at  $T_{\text{stable}}$ . Slides were stored and transported under liquid nitrogen, including transfer to the low temperature mount of a Picker biplanar x-ray diffractometer.

Two experiments established that the coordination of the TaS<sub>2</sub> layers does not change in the intercalation process. The original 1T-TaS<sub>2</sub> phase is stable above 700 °C<sup>12</sup>; the 4Hb-TaS<sub>2</sub> between 500 and 700 °C<sup>8</sup>; and the 2H-TaS<sub>2</sub> below about 450 °C. The 1T and 4Hb phases may be obtained by quenching them from the high temperature growth zone where they are stable down to room temperature merely by removing the quartz tubes from the furnace. The possibility always exists in a metastable system that the crystal will transform to the stable 2H phase upon intercalation. The sequence of x-ray diffraction spectra shown in Fig. 2 was carried out to verify that the 4Hb coordination remains after the intercalation reaction and the subsequent deintercalation. It follows from the presence of the  $(10\bar{5})$  line in Fig. 2c, as well as the values of the  $a$  and  $c$  parameters, that this is still the 4Hb structure. Ethylamine was chosen for this experiment since samples made with it show the least degradation after deintercalation.

A similar sequence, shown in Fig. 3, was used to show that the 1T-TaS<sub>2</sub> coordination does not transform with intercalation. The sample was deintercalated under vacuum at 150 °C for 5 min. The deintercalated sample remains in the 1T phase, as shown by the x-ray diffraction in Fig. 3 and from the  $a$  and  $c$  parameters.

Intercalation is normally accompanied by a shift of the lateral registry of the layers.<sup>13</sup> The absence of the  $(100)$  and the intensity distribution of the  $(10\bar{L})$  and  $(11\bar{L})$  diffraction lines in Figs. 2b and 3b indicate that the TX<sub>2</sub> layers are shifted by  $a/\sqrt{3}$  relative to each other along  $(11\bar{2}0)$  plane.<sup>13</sup> A study of the intensity distribution yielded the most probable structures, shown in Fig. 4, for 2H-, 4Hb-, and 1T-TaS<sub>2</sub> intercalated with ammonia and EDA. However, Patterson intensity analyses have not been carried out.

The crystal field produced by the sulfur atoms in the intercalated layers of the 2H and 4Hb complexes is trigonal prismatic. This similarity suggests that the bonding interaction is the same in these complexes. The crystal field produced by the sulfur atoms in 3R-TaS<sub>2</sub>(EDA)<sub>1/4</sub> is octahedral, as shown in Fig. 4, and is similar to intercalated compounds of 1T-TaS<sub>2</sub><sup>14</sup> and of alkali metals in 1T-ZrS<sub>2</sub><sup>15</sup> and 1T-TiS<sub>2</sub>.<sup>16</sup> In this structure the transition element faces a chalcogen across the van der Waals gap.

The crystal structure parameters of NbSe<sub>2</sub> cyclopropylamine complex were difficult to obtain owing to a serious degradation by the amine, resulting in very broad lines and several  $c$  spacings. Of three samples studied, only the one reported in Table I had a sufficiently well-defined  $c$  spacing to allow analysis.

### III. METHOD OF MEASUREMENT

Superconductivity was detected by measuring the response to an applied ac field. The susceptibility appara-

TABLE I. Parameters of some intercalated layered materials.

Intercalate	Layered material	$T_c^a$ (°K)	$a$ (Å)	$c$ (Å)	$\delta$ (Å)	Stoic.	$T_{stable}$ (°C)	$T_{interc}$ (°C)
	1T-TaS <sub>2</sub>	...	3.346 <sup>b</sup>	5.860 <sup>b</sup>				
	2H-TaS <sub>2</sub>	0.8	3.310	2×6.040				
	4Hb-TaS <sub>2</sub>	<1.1	3.328	4×5.929				
	2H-NbSe <sub>2</sub>	7.2	3.449	2×6.272				
	2H-TaSe <sub>2</sub>	0.15 <sup>d</sup>	3.436 <sup>b</sup>	2×6.348 <sup>b</sup>				
	4Ha-NbSe <sub>2</sub>	6.3	3.433 <sup>c</sup>	4×6.303 <sup>c</sup>				
NH <sub>3</sub> <sup>e</sup> (Ammonia)	2H-TaS <sub>2</sub>	3.8	3.319	2×9.104	3.064	1	25	25
	4H-TaS <sub>2</sub>	5.0	3.338	4×9.263	3.334	1	-40	25
	2H-NbSe <sub>2</sub>	0.6	3.460	2×9.675	3.403	1	-40	100
CH <sub>3</sub> NH <sub>2</sub> <sup>e</sup> (Methylamine) (MeA)	2H-TaS <sub>2</sub>	5.6	3.324	2×9.236	3.211	$\frac{1}{2}$	25	25
	4H-TaS <sub>2</sub>	4.6	3.344	4×9.301	3.372	$\frac{1}{2}$	-20	25
	2H-NbSe <sub>2</sub>	0.95	3.458	2×9.861	3.589	$\frac{1}{2}$	-20	100
CH <sub>3</sub> CH <sub>2</sub> NH <sub>2</sub> <sup>e</sup> (Ethylamine) (EtA)	2H-TaS <sub>2</sub>	3.4	3.322	2×9.562	3.537	$\frac{1}{2}$	25	50
	4H-TaS <sub>2</sub>	3.5	3.329	4×9.514	3.585	$\frac{1}{2}$	0	25
	2H-NbSe <sub>2</sub>	1.20	3.449	2×9.877	3.605	$\frac{1}{2}$	0	100
(CH <sub>3</sub> ) <sub>2</sub> NH <sup>e</sup> (Dimethylamine)	2H-TaS <sub>2</sub>	3.4	3.320	2×9.585	3.560		25	110
	4H-TaS <sub>2</sub>	3.8	3.335	4×9.893	3.964		-20	110
	2H-NbSe <sub>2</sub>	3.0	3.454	2×10.228	3.956		-20	110
(CH <sub>3</sub> CH <sub>2</sub> ) <sub>3</sub> N <sup>e</sup> (Triethylamine)	2H-TaS <sub>2</sub>	<1.3	3.317	2×10.087	4.062		25	55
	4H-TaS <sub>2</sub>	1.3	...	4×9.96	4.03		25	25
	2H-NbSe <sub>2</sub>	<1.3	3.45	2×10.14	3.87		25	55
NH <sub>2</sub> CH <sub>2</sub> CH <sub>2</sub> NH <sub>2</sub> (Ethylenediamine) (EDA)	2H-TaS <sub>2</sub>	4.7	3.323	2×9.527	3.502	$\frac{1}{4}$	25	150
	4H-TaS <sub>2</sub>	3.2	3.346	4×9.770	3.841	$\frac{1}{4}$	25	100
	2H-NbSe <sub>2</sub>	<0.35	3.453	2×10.241	3.969	$\frac{1}{4}$	25	150
	1T-TaS <sub>2</sub>	<0.35	3.370	3×9.729	3.869	$\frac{1}{4}$	25	150
	2H-TaSe <sub>2</sub>	0.95	3.439	2×10.219	3.871	$\frac{1}{4}$	25	150
	4H-NbSe <sub>2</sub>	1.05	3.444	4×10.235	3.932		25	150
C <sub>3</sub> H <sub>5</sub> NH <sub>2</sub> (Cyclopropylamine)	2H-TaS <sub>2</sub>	3.0	3.315	2×10.241	4.216		25	50
	2H-NbSe <sub>2</sub>	1.1	3.455	2×10.740	4.468		25	50
C <sub>5</sub> H <sub>9</sub> NH <sub>2</sub> (Cyclopentylamine)	4H-TaS <sub>2</sub>	3.15	3.319	4×15.655	9.726		-25	25
	2H-NbSe <sub>2</sub>	0.90	3.458	2×15.192	8.920		-25	50
C <sub>5</sub> H <sub>5</sub> N (Pyridine) (Pyr)	2H-TaS <sub>2</sub> <sup>f</sup>	3.6	3.326	2×11.85 2×12.02	5.81 5.98	$\frac{1}{2}$	25	200
	4H-TaS <sub>2</sub>	3.2	3.365	4×11.846	5.917	$\frac{1}{2}$	-30	150

<sup>a</sup>0.4°K ≤ ΔT ≤ 0.6°K for all samples.<sup>b</sup>Reference 1.<sup>c</sup>Reference 23.<sup>d</sup>M. H. van Maaren and G. M. Schaffer, Phys. Lett. A 24, 645 (1967).<sup>e</sup>X-ray data obtained at 77°K.<sup>f</sup>T<sub>c</sub> and x-ray data from Ref. 4.

tus used for measurements above 1.4°K was of the high frequency, self-inductance type.<sup>17</sup> Samples superconducting below 1.4°K were measured in a low-frequency mutual inductance ac susceptibility apparatus operating in a He<sup>3</sup> cryostat.<sup>9</sup> In both systems,  $T_c$  is defined as the peak of out-of-phase signal, usually 0.1–0.2°K below the onset of diamagnetic shift in the in-phase susceptibility owing to the presence of superconducting shielding. No appreciable thermal hysteresis was observed in these samples, but all transitions of intercalated complexes were of the order of 0.5°K in width.

The electrical resistivities with the current parallel to the plane of the layers ( $\rho_a$ ) were measured as a function of temperature using an ac van der Pauw technique<sup>18</sup> on intercalated single crystals, while the data with the current normal to the plane ( $\rho_c$ ) were taken using an ac

four-probe method, assuming  $\rho_o \gg \rho_a$ . The temperature dependence is accurate to ±2%, while the magnitude is limited to ±10%. This latter uncertainty arises from the difficulty in measuring the dimensions of the irregularly shaped crystals. Further, the magnitude of  $\rho_c$  should be treated with caution since unnoticed cleavage between the layers can influence the magnitude enormously. The values reported in Table II represent an average of several samples in each case, all falling within the quoted uncertainty.

The heat capacity data reported in Table III were taken using a silicon bolometer calorimeter system described elsewhere.<sup>19,20</sup> The sample is mounted with a thin layer of thermally conducting grease onto a silicon chip bolometer. The bolometer is suspended via gold-copper electrical leads. These leads thermalize the sample and

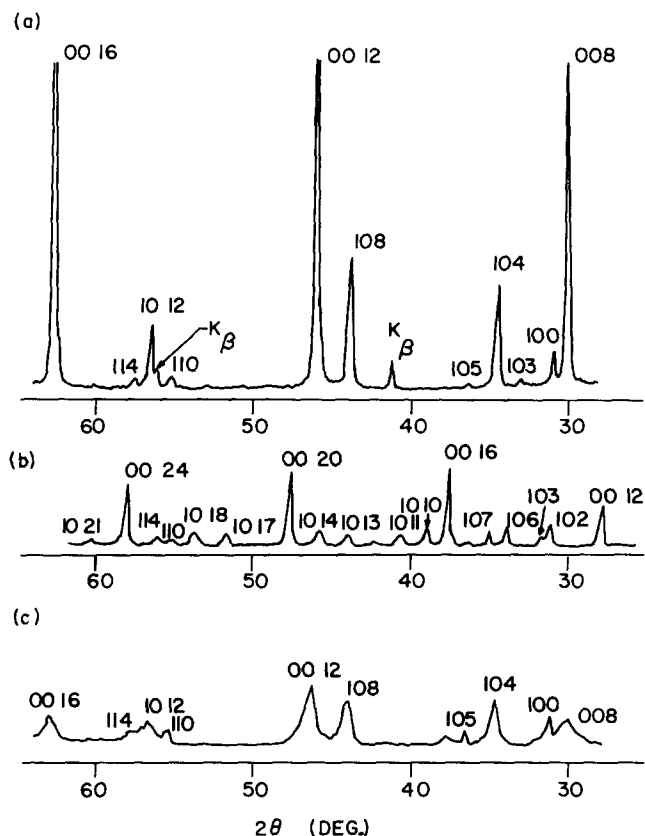


FIG. 2. X-ray study of 4H-TaS<sub>2</sub> showing spectra for  $28^\circ < 2\theta < 65^\circ$  for (a) 4H-TaS<sub>2</sub>, (b) 4H-TaS<sub>2</sub>(EtA)<sub>1/2</sub>, and (c) deintercalated 4H-TaS<sub>2</sub>(EtA)<sub>1/2</sub> showing return to the 4H-TaS<sub>2</sub> structure by the presence of (105) and the *a* and *c* parameters. The incomplete deintercalation of (c) is shown by the remnant of intercalation (00 16) to the left of (105) and by the width of the (001) lines.

bolometer to a reference block with about a three-second time constant. To measure  $C_v(T_0 + 0.01^\circ\text{K})$ , where  $T_0$  is the reference block temperature, the sample temperature is incremented  $0.02^\circ\text{K}$  above that of the block, and then allowed to decay. A Nicolet 1070 signal averaging computer measures this exponential decay, and an on-line PDP-8/e computer calculates the time constant of the decay. The total heat capacity is then calculated using the known thermal conductivity of the wires. The sample heat capacity is derived from the measured total heat capacity by subtraction of the heat capacity of the bolometer and grease. The measured parameters in the Debye-Sommerfeld relation  $C = \gamma T + \beta T^3$  are given in Table III. The samples used in this experiment were in the 15–25 mg range, with a typical instrumental addendum of about 15% of the total heat capacity at  $1^\circ\text{K}$  and 25% at  $5^\circ\text{K}$ . The deviation in the data was  $\pm 2\%$  or less. The accuracy of the calorimeter has been established by comparison with standard germanium with reproducible results within  $\pm 2\%$ .<sup>20</sup>

## IV. RESULTS AND DISCUSSION

### A. Superconductivity

The highest transition temperature observed in the dichalcogenides is that of NbSe<sub>2</sub>, as can be seen in Table

I. The NbSe<sub>2</sub> intercalation complexes show either no superconductivity above  $0.35^\circ\text{K}$  (EDA) or  $T_c$ 's markedly below the  $7.2^\circ\text{K}$   $T_c$  of NbSe<sub>2</sub>. The original 4Hb-TaS<sub>2</sub> transported crystals showed quite broad transitions into the superconducting state as measured by ac susceptibility, typical of what is frequently observed when connected filaments of a minor superconducting phase are imbedded in a major nonsuperconducting phase. If the distribution of the minor phase is topologically suitable, filamentary superconductivity can provide complete flux exclusion and thus give a full in-phase signal when as little as  $\sim 1$  at.% of the minor phase is present. However, the minor phase can contribute to the heat capacity only in proportion to its atomic fraction. No sign of superconductivity was detected in the heat capacity of 4Hb-TaS<sub>2</sub> crystals down to  $1.1^\circ\text{K}$ . However, the intercalation complexes have transitions varying up to  $5^\circ\text{K}$ , as given in Table I. The 2H polymorphs of TaS<sub>2</sub> and TaSe<sub>2</sub> are each seen to increase in  $T_c$  by about a factor of 6 to 4.7 and  $0.95^\circ\text{K}$ , respectively, upon formation of the EDA intercalation complex.

### B. Resistivity

The temperature dependence of the resistivity has been investigated for three of the layered materials studied here. Table III summarizes the room temperature resistivities and anisotropies as well as the residual re-

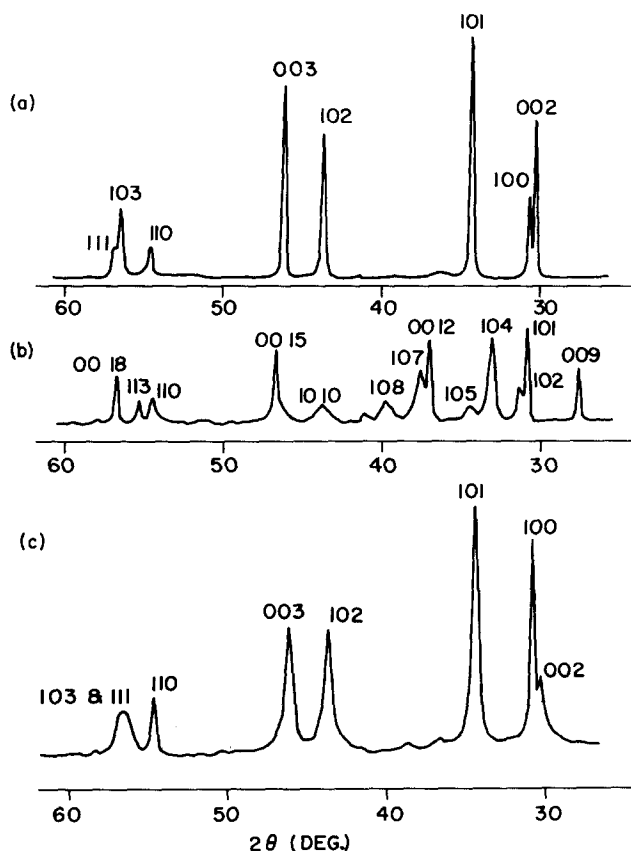


FIG. 3. X-ray study of octahedral TaS<sub>2</sub> showing spectra for  $25^\circ < 2\theta < 60^\circ$  for (a) 1T-TaS<sub>2</sub>, (b) 3R-TaS<sub>2</sub>(EDA)<sub>1/4</sub>, and (c) deintercalated 3R-TaS<sub>2</sub>(EDA)<sub>1/4</sub> showing return to 1T-TaS<sub>2</sub> by the *a* and *c* parameters. Incomplete deintercalation is shown by the line width.

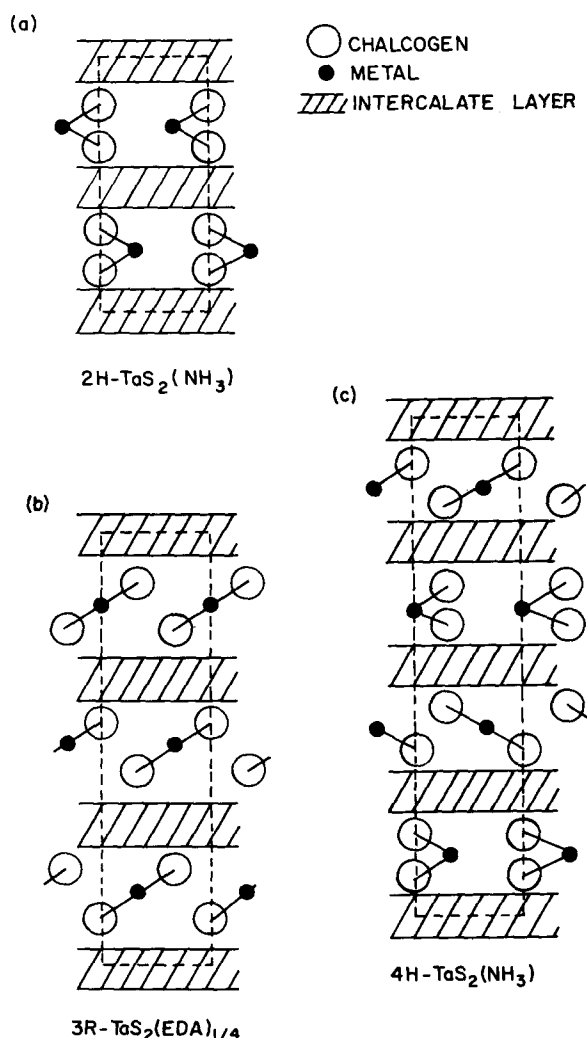


FIG. 4. Crystal structures for intercalated compounds shown along the (11 $\bar{2}$ 0) plane (compare Fig. 1) deduced from intensity distributions of (10 $\bar{l}$ ) and (11 $\bar{l}$ ) lines for (a) 2H-TaS<sub>2</sub>(NH<sub>3</sub>) and 2H-NbSe<sub>2</sub>(NH<sub>3</sub>), (b) 3R-TaS<sub>2</sub>(EDA)<sub>1/4</sub> (intercalated 1T-TaS<sub>2</sub>), and (c) 4H-TaS<sub>2</sub>(NH<sub>3</sub>). Note the similarity of the van der Waals gap in (a) and (c).

sistance ratios.

In Fig. 5, the resistivity of NbSe<sub>2</sub><sup>21</sup> is compared with the resistivity of NbSe<sub>2</sub>(EDA)<sub>1/4</sub>. The anisotropy of NbSe<sub>2</sub> has a constant value of 30 to below 100 °K, and therefore only  $\rho_c$  is shown. The normalized resistivities show that intercalation has altered the temperature dependence in several ways: (1) The region above 100 °K in both materials can be described reasonably well by straight lines of different slope suggesting phonon scattering is the dominant mechanism. (2) Below 100 °K, the resistivity of NbSe<sub>2</sub> first decreases with a greater slope than above 100 °K, and then flattens out near 25 °K until it becomes superconducting at 7 °K. By comparison, NbSe<sub>2</sub>(EDA)<sub>1/4</sub> has no bend near 100 °K and shows a resistance minimum near 25 °K in both  $\rho_c$  and  $\rho_a$ . (3) Even though the anisotropy increases by a factor of 5 upon intercalation, the ratio  $\rho_c/\rho_a$  shows less temperature dependence than found in the unintercalated crystals which itself is quite moderate.

In Fig. 6, 4Hb-TaS<sub>2</sub> is compared with 4H-TaS<sub>2</sub>(EDA)<sub>1/4</sub>. In contrast to NbSe<sub>2</sub>, 4Hb-TaS<sub>2</sub> shows a clear difference between the temperature dependence of  $\rho_c$  and  $\rho_a$ .<sup>8</sup> The changes introduced by intercalation are (1) an increase in  $\rho_c$  by almost two orders of magnitude, and (2) a suppression of the structure in the resistivity below 100 °K in  $\rho_c$ , although the shoulder is still present in the complex. Irreversible effects in 4H-TaS<sub>2</sub>(EDA)<sub>1/4</sub> prevented resistivity measurements above room temperature from being used to investigate the transition observed in the unintercalated material at 315 °K.

Intercalation of EDA into 1T-TaS<sub>2</sub> has a very pronounced effect on the temperature dependence of  $\rho_a$ , shown in Fig. 7. The 1T phase shows transitions in the resistivity, a metal-semiconductor transition at 350 °K, and a semiconductor-to-semiconductor transition at 190 °K.<sup>12</sup> We observed that the resistivity of 3R-TaS<sub>2</sub>(EDA)<sub>1/4</sub> shows the low temperature transition has been suppressed by intercalation, while the high temperature transition has only moved to a slightly lower temperature of 330 °K. The coincidence of magnitudes of resistivities at low  $T$  and 330 °K in the original phase and in the complex is striking. However, below 10 °K the resistivity of the complex becomes temperature independent, while that for the 1T-TaS<sub>2</sub> continues to rise.

### C. Heat capacity

The data for the systems given in Table III show that the trend already observed in 2H-TaS<sub>2</sub> of a pronounced decrease in the Debye temperature,  $\theta_D$ , upon intercalation<sup>22</sup> is also present. This increase in the lattice heat capacity has been attributed at least in part to the low energy degrees of freedom associated with the intercalated organic layer. Onset of a  $T^2$  behavior of  $C$  is observed at a lower temperature for the complex than for the parent phase.

In the 2H-NbSe<sub>2</sub> and 4Hb-TaS<sub>2</sub> systems,  $\gamma$  and  $T_c$  change in the same direction. The McMillan formulation of the theory of superconductivity for strong coupled superconductors<sup>24</sup> provides some insight into the physical properties. The decrease in  $\lambda_{\text{McMillan}}$ , defined in Table III, with intercalation in 2H-NbSe<sub>2</sub> is consistent with the decrease in  $dp/dT$  shown in Fig. 5.

It is possible that the disappearance of portions of the Fermi surface upon superlattice formation in 1T

TABLE II. Resistivity data.

Compound	$\rho_c$ (300 °K) $\Omega - \text{cm}$	$\rho_a$ (300 °K) $\Omega - \text{cm}$	$\rho_c/\rho_a$ (300 °K)	$\rho_c$ (300 °K) $\rho_a$ (4 °K)	$\rho_c$ (300 °K) $\rho_c$ (4 °K)
2H-NbSe <sub>2</sub> <sup>a</sup>	$5 \times 10^{-3}$	$1.6 \times 10^{-4}$	30	20	10
2H-NbSe <sub>2</sub> (EDA) <sub>1/4</sub>	0.12	$8.6 \times 10^{-4}$	140	1.6	1.8
4Hb-TaS <sub>2</sub> <sup>b</sup>	$6 \times 10^{-3}$	$4 \times 10^{-4}$	15	50	~1
4H-TaS <sub>2</sub> (EDA) <sub>1/4</sub>	0.3	$6.4 \times 10^{-4}$	450	4	~1
1T-TaS <sub>2</sub> <sup>c</sup>		$8.3 \times 10^{-4}$			
3R-TaS <sub>2</sub> (EDA)		$1.5 \times 10^{-3}$			
2H-TaS <sub>2</sub> <sup>d</sup>	$2 \times 10^{-3}$	$1.5 \times 10^{-4}$	10	20	6
2H-TaS <sub>2</sub> (Pyr) <sub>1/2</sub> <sup>d</sup>	2–20	$3 \times 10^{-4}$	$10^4$	5	3

<sup>a</sup>Reference 21.

<sup>b</sup>Reference 8.

<sup>c</sup>Reference 12.

<sup>d</sup>Reference 35.

TABLE III. Heat capacity data.

Compound	$T_c$ (°K)	$\gamma$ $mJ/m_0(^{\circ}K)^2$	$\beta$ $mJ/m_0(^{\circ}K)^4$	$\theta_D$ (°K)	$\lambda_{McM}^a$	$N_{BS}(0)^a$ $eV^{-1} \cdot \text{molecule}^{-1}$	$\frac{\Delta C}{\gamma T_c}$
1T-TaS <sub>2</sub> <sup>b</sup>	...	$1.4 \pm 0.1$	$0.38 \pm 0.02$	172	...	...	...
2H-TaS <sub>2</sub> <sup>c</sup>	$0.8^d$	$8.5 \pm 0.1$	0.37	174	0.51	1.19	1.9
2H-TaS <sub>2</sub> (Pyr) <sub>1/2</sub> <sup>c</sup>	3.4	$9.1 \pm 0.2$	2.32	94	0.89	1.02	0.96
4Hb-TaS <sub>2</sub> <sup>e</sup>	$< 1.1$	$2.9 \pm 0.2$	0.38	172	$< 0.54^e$	$0.4 < N < 0.6$	...
4H-TaS <sub>2</sub> (EDA) <sub>1/4</sub>	3.2	$8.1 \pm 0.2$	0.89	130	0.77	0.97	0.4
2H-NbSe <sub>2</sub> <sup>c</sup>	7.1	$16.5 \pm 0.5$	0.53	154	1.02	1.73	2.1
2H-NbSe <sub>2</sub> (EDA) <sub>1/4</sub> <sup>e</sup>	$< 0.35^d$	$7.4 \pm 0.2$	1.03	123	$< 0.46^e$	$1.1 < N < 1.6$	...
Pb	7.19	...	...	...	...	...	2.65
BCS	...	...	...	...	...	...	1.43

<sup>a</sup>The McMillan formalism was derived to fit the experimental data for transition metal superconductors using the measured phonon spectrum of niobium, according to Refs. 13 and 22. The accuracy of this calculation for layered materials is therefore open to question. The analog of the BCS equation for  $T_c$  is given by

$$T_c = \frac{\theta_D}{1.45} \exp \left[ -\frac{1.04(1+\lambda)}{\lambda - \mu^*(1+0.62\lambda)} \right],$$

or inverted form

$$\lambda = \frac{1.04 + \mu^* \ln(\theta_D/1.45 T_c)}{(1 - 0.62\mu^*) \ln(\theta_D/1.45 T_c) - 1.04},$$

where  $\mu^*$  is the screened Coulomb repulsion, and  $\lambda$  the electron-phonon coupling constant.  $\lambda$  is given by  $\lambda = N(0) \langle I^2 \rangle / M \langle \omega_q^2 \rangle$ , where  $N(0)$  is the band structure density of states,  $\langle I^2 \rangle$  an average of the electron-phonon matrix elements, and  $\langle \omega_q^2 \rangle$  an effective, average phonon frequency. The electronic coefficient of the specific heat is renormalized by  $(1+\lambda)$  and related to the density of states by  $\gamma = \frac{2}{3} \pi^2 k_B^2 (1+\lambda) N(0)$ . Values of  $\lambda$  were calculated with an assumed value of  $\mu^* = 0.15$ , as suggested by McMillan for transition metal superconductors.

<sup>b</sup>Reference 7.

<sup>c</sup>Reference 23.

<sup>d</sup> $T_c$  from ac susceptibility measurement.

<sup>e</sup>For two of the materials, only upper limits can be placed on  $T_c$ , leading to an upper limit for  $\lambda$ . Using the upper limit, and assuming a lower limit of  $\lambda = 0$ , the range for  $N(0)$  can be calculated.

and 4Hb-TaS<sub>2</sub><sup>2</sup> is responsible for their small  $\gamma$  values. The  $\gamma$  observed for the 4Hb polymorph (Table III) is smaller than the average of the 1T and 2H polymorphs.

Since the 4Hb polymorph consists of a combination of the 1T and 2H polymorphs, in the limit of zero interaction between adjacent layers one would expect

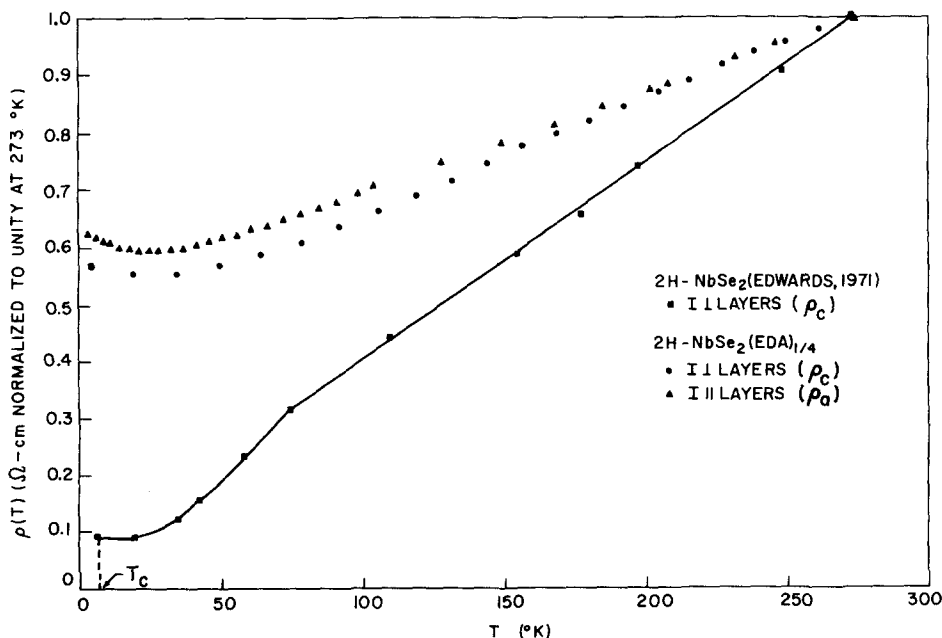
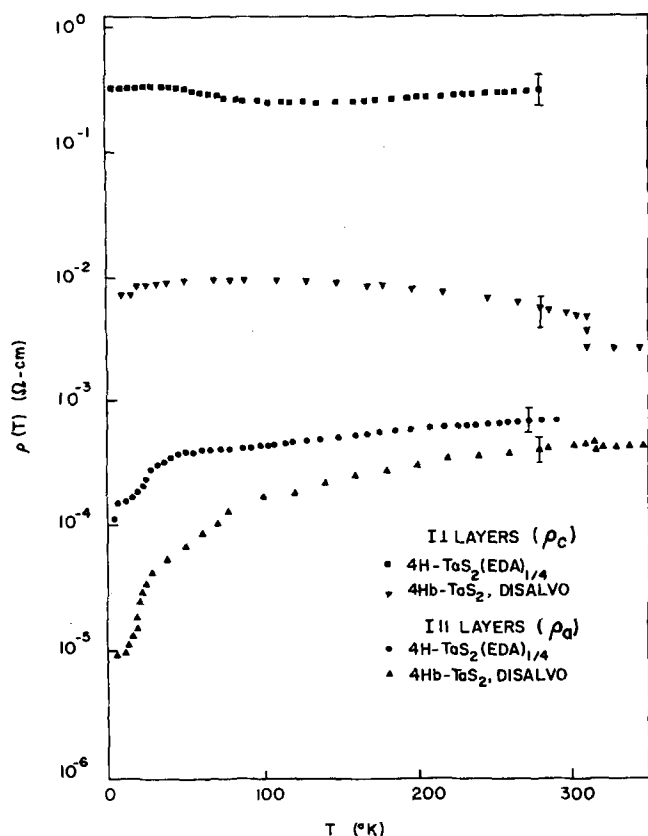
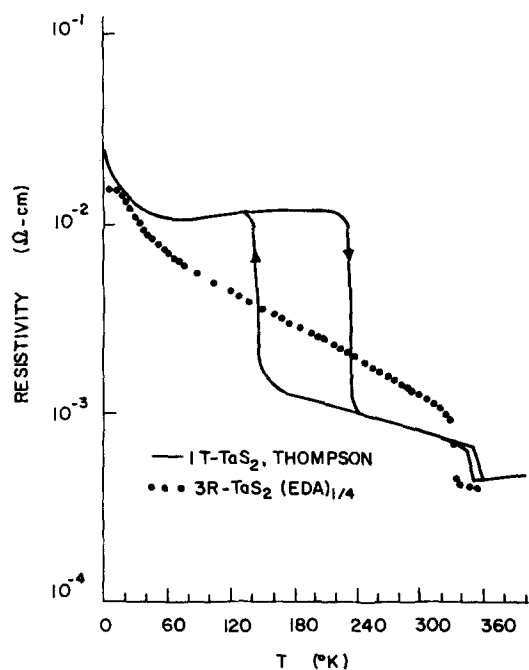
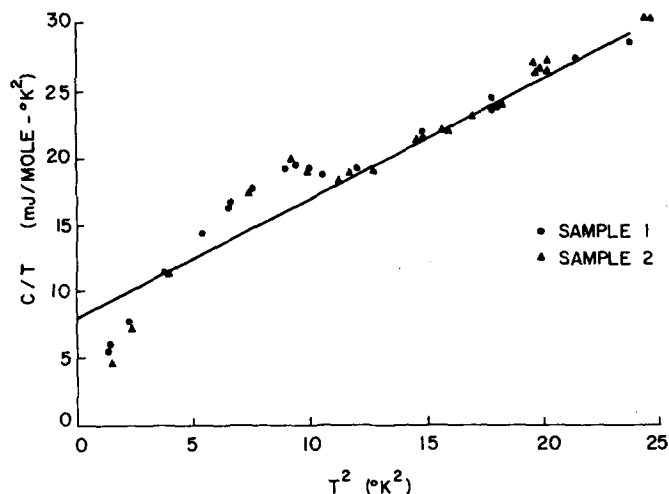


FIG. 5. Resistivity of 2H-NbSe<sub>2</sub>(EDA)<sub>1/4</sub> and 2H-NbSe<sub>2</sub> (Ref. 21) normalized to unity at 273°K.  $\rho_a$  and  $\rho_c$  for NbSe<sub>2</sub> are proportional.



FIG. 6. Resistivity of 4Hb-TaS<sub>2</sub> (Ref. 8) and 4H-TaS<sub>2</sub>(EDA)<sub>1/4</sub>.

various physical quantities for 4Hb-TaS<sub>2</sub> to correspond to an average of those for the 1T and 2H phases. The *a*-axis spacing for the 4Hb phase is exactly the mean of that of the parent phases (Table I), while the relative

FIG. 7. Resistivity along the *a* axis of 1T-TaS<sub>2</sub> (Ref. 12) and 3R-TaS<sub>2</sub>(EDA)<sub>1/4</sub>. The 1–10 °K temperature region of 3R-TaS<sub>2</sub>(EDA)<sub>1/4</sub> is temperature independent.FIG. 8. Specific heat of 4H-TaS<sub>2</sub>(EDA)<sub>1/4</sub> for two samples. Extrapolation of both curves suggests a nonzero intercept suggesting the presence of normal electrons.

*c*-axis spacing is closer to that of the 1T phase. Freshly transported crystals of 4Hb-TaS<sub>2</sub> showed filamentary superconducting transitions as measured by ac susceptibility between 1 and 4 °K in nearly all cases, as already discussed. The heat capacity did show a positive deviation from the conventional linear heat capacity plot of *C/T* vs *T*<sup>2</sup> as the temperature decreased below 3 °K. A similar deviation has been observed below 2 °K<sup>25</sup> in 1T-TaS<sub>2</sub>, which of course has no superconducting transition. An applied magnetic field of 8 kG has no apparent effect in either case. The deviation could be accounted for by a small concentration ( $\leq 0.1\%$ ) of paramagnetic centers perhaps associated with imperfections in the crystals.

The heat capacity of two samples of 4H-TaS<sub>2</sub>(EDA)<sub>1/4</sub> is shown in Fig. 8. Three pertinent observations are made. (1) The values of  $\gamma$  for the intercalated compound increases more than a factor of 2 (Table III) and is comparable with that of an intercalation complex of 2H-TaS<sub>2</sub> with a corresponding *T*<sub>c</sub>. (2) A broad anomaly is observed centered around 3.2 °K indicating the formation of a condensed, superconducting state. The width of the transition, of the order of 0.5 °K, is comparable to widths for other intercalated TaS<sub>2</sub> complexes. However, the size of the jump in the heat capacity is smaller than previously observed in the 2H-TaS<sub>2</sub> complexes.<sup>22</sup> (3) An extrapolation of the heat capacity below *T*<sub>c</sub> to zero temperature in the one sample for which more than two points are available indicates a nonzero intercept. An explanation for the finite intercept would be that a fraction of the sample remains normal below *T*<sub>c</sub> because it is not complexed with the EDA. However, we reject this explanation because a fraction greater than 20% of the sample would have to be unintercalated to account for the size of the finite intercept at *T* = 0, and only one phase is observed in x-ray diffraction.

## V. CONCLUSIONS

The experimental observations lead to the following conclusions:

(1) A charge transfer model does qualitatively account for the stability of the complexes studied. The stabilization of a Mulliken electron donor-acceptor complex is due to the admixture of excited charge transfer configurations into the ground covalent configuration.<sup>5</sup> For a given ligand, the variation in binding energy and therefore stability is primarily due to the properties of the dichalcogenide. A comparison of  $T_{\text{stable}}$  shown in Table I clearly shows that for all compounds studied, 2H-TaS<sub>2</sub> was more stable than 4H-TaS<sub>2</sub> and 2H-NbSe<sub>2</sub>. In all cases, the complexes are stable in the presence of excess liquid in equilibrium with the vapor, but only the 2H phase complexes are sufficiently stable at room temperature to resist changes in entropy which favor deintercalation. The relative thickness of intercalated NH<sub>3</sub> layers is given by the parameter  $\delta$  in Table I. In the NH<sub>3</sub> complexes,  $\delta$  is approximately 10% greater for 4H-TaS<sub>2</sub>(NH<sub>3</sub>) and 2H-NbSe<sub>2</sub>(NH<sub>3</sub>) than for 2H-TaS<sub>2</sub>(NH<sub>3</sub>). This contraction of the intercalate layer in the more stable complex is consistent with a higher binding energy in the charge transfer model.<sup>5</sup>

(2) When minima in  $\rho_a$  and  $\rho_c$  vs  $T$  are observed, the superconductivity is suppressed to below 0.35 °K. Such minima have been observed in NbSe<sub>2</sub>(EDA)<sub>1/4</sub> and also in 4H-TaS<sub>1.6</sub>Se<sub>0.4</sub>(aniline)<sub>1/4</sub>.<sup>7</sup> The fact that Thompson<sup>26</sup> found a resistance minimum in specially treated TaS<sub>2</sub>(pyridine)<sub>1/2</sub> along the  $c$  axis but not in the  $a$  axis, and also found the superconductivity to remain, can be attributed to the huge anisotropy and two-dimensional character of the complex. The occurrence of a resistance minimum is frequently associated with Kondo (spin-dependent) scattering, which also tends to destroy superconductivity. While it is unlikely that paramagnetic impurities are causing the Kondo scattering, the possibility that a small fraction of bonds are broken by chalcogen extraction during the intercalation progress and are turned into defects capable of Kondo scattering cannot be ruled out. A number of other more speculative mechanisms deserve further investigation. A phonon-assisted, hopping conductivity<sup>27</sup> through the intercalate layer is an intrinsic mechanism that could result in a low temperature minimum in the resistivity.<sup>28</sup> Another possibility is that there may be some instability driven by a Fermi wave vector of the type observed at higher temperatures in nonintercalated compounds.<sup>2</sup> Such instabilities can give charge density waves which can grow with decreasing temperature.<sup>29</sup>

(3) The increase in  $\rho_c$  upon intercalation of 4Hb-TaS<sub>2</sub> can be explained by the model of tunneling through a barrier. The resistivity of 4Hb-TaS<sub>2</sub> complexes in Fig. 6 does not appear to be dominated by mixing the resistivities, as occurs in NbSe<sub>2</sub>(EDA)<sub>1/4</sub> and TaS<sub>2</sub>(pyridine)<sub>1/2</sub>. The relatively temperature-independent conductivity suggests that the dominant conduction mechanism in 4Hb-TaS<sub>2</sub> in  $\rho_c$  is due to tunneling. A tunneling conductivity involves a transition probability

$$P \sim \exp(-2\mu\delta) \quad (1)$$

leading to a resistivity of the form

$$\rho_c \sim \exp(2\mu\delta) \quad (2)$$

with a barrier height given by  $\hbar^2\mu^2/2m$ . The observed

change in  $\rho_c$  upon intercalation of 4Hb-TaS<sub>2</sub> is a factor of 50. A lattice expansion of  $\delta = 3.5$  Å leads to a characteristic tunneling length  $\mu^{-1} \sim 1.7$  Å. The effective mass is not known; however, an  $\sim 2$  eV barrier is reasonable for tunneling through a dielectric medium. Confirmation of the nature of the conductivity would involve experiments such as resistivity under pressure to observe the exponential dependence.

(4) The fact that the phase transition in 1T-TaS<sub>2</sub> at 350 °K is not greatly affected by the separation and lateral translation of the disulfide layers upon intercalation suggests that it is an intralayer transition, perhaps involving the formation of superlattices within each layer.<sup>2</sup> The disappearance of the transition at 190 °K suggests a dependence upon interlayer coupling.

(5) The apparent finite intercept of  $C/T$  vs  $T^2$  observed for the 4Hb-TaS<sub>2</sub>(EDA) complexes in Fig. 8 is suggestive of gapless superconductivity.<sup>30</sup> Since  $\rho_a$  and  $\rho_b$  in the 4Hb complexes are not dominated by shorts, there could be normal Bloch states in the superconducting energy gap for electrons constrained to propagate in the octahedral layers.

Finally, (6) the formation of charge transfer NbSe<sub>2</sub> complexes can explain the observed reduction in  $T_c$ . Band structure calculations<sup>31,32</sup> show that the Fermi level lies near a very sharp peak in the density of states; the calculations are supported by the photoemission spectroscopic results<sup>32,33</sup> which show  $N(0)$  decreasing rapidly with energy at the Fermi level. Changes produced by intercalation on the joint density of states have been made evident by the shifts observed in the optical absorbancy peaks when NbSe<sub>2</sub> intercalated complexes are formed.<sup>34</sup> Therefore, the finite perturbation introduced by the ligands, which leads to the reduction of  $T_c$ , must decrease  $N(0)$ .

## ACKNOWLEDGMENTS

We wish to thank Dr. R. E. Schwall for making his specific heat data available to us prior to publication. Also, we thank A. Carpenter and C. Staar for their help in the laboratory.

\*Research was supported by the Air Force Office of Scientific Research, Air Force Systems Command, USAF, under Grant No. AFOSR 73-2435. This work was presented in partial fulfillment of the Ph.D. dissertation requirement of S. F. Meyer, Stanford University, 1973.

†Permanent address: Department of Physics, University of Illinois, Urbana, ILL 61801.

‡Permanent address: Department of Chemistry, San José State University, San José, CA 95192.

<sup>1</sup>F. Hulliger, in *Structure and Bonding*, edited by C. Jorgensen (Springer-Verlag, Berlin, 1968), Vol. 4; J. A. Wilson and A. D. Yoffe, *Adv. Phys.* **18**, 193 (1969).

<sup>2</sup>J. A. Wilson, F. J. Di Salvo, and S. Mahajan, *Phys. Rev. Lett.* **32**, 882 (1974); P. M. Williams, G. S. Parry, and C. P. Scruby, *Philos. Mag.* **29**, 695 (1974).

<sup>3</sup>F. R. Gamble, F. J. Di Salvo, R. A. Klemm, and T. H. Geballe, *Science* **168**, 568 (1970); F. R. Gamble and T. H. Geballe, in *Treatise on Solid State Chemistry*, edited by N. B. Hannay (Plenum, New York, 1974).

<sup>4</sup>F. R. Gamble, J. H. Osiecki, and F. J. Di Salvo, *J. Chem.*

- Phys. **55**, 3525 (1971).
- <sup>5</sup>J. V. Acrivos, S. F. Meyer, and T. H. Geballe, in *Electrons in Fluids*, edited by J. Jortner and N. R. Kestner (Springer-Verlag, New York, 1973), p. 341.
- <sup>6</sup>E. Ehrenfreund, A. C. Gossard, and F. R. Gamble, Phys. Rev. B **5**, 1708 (1972).
- <sup>7</sup>J. A. Benda, R. E. Howard, and W. A. Phillips, J. Phys. Chem. Solids **35**, 937 (1974); J. A. Benda, Phys. Rev. B **10**, 1409 (1974).
- <sup>8</sup>F. J. Di Salvo, B. G. Bagley, J. M. Voorhoeve, and J. V. Waszczak, J. Phys. Chem. Solids **34**, 1257 (1973).
- <sup>9</sup>F. J. Di Salvo, Ph.D. dissertation, Stanford University, 1971 (unpublished); H. Schaefer, *Chemical Transport Reactions* (Academic, New York, 1964).
- <sup>10</sup>J. V. Acrivos and K. S. Pitzer, J. Phys. Chem. **66**, 1693 (1972).
- <sup>11</sup>It is true that cyclopropylamine complexes of NbSe<sub>2</sub> and TaS<sub>2</sub> are already known [S. F. Meyer, T. H. Geballe, and J. V. Acrivos, Bull. Am. Phys. Soc. **17**, 519 (1972); S. F. Meyer, Ph.D. dissertation, Stanford University, 1973 (unpublished)]. However, solvents, such as dichloromethane, will extract cyclopropylamine from NbSe<sub>2</sub>, indicating that it is not tightly bound. EDA is not extracted from the complex by any solvent yet tried.
- <sup>12</sup>A. H. Thompson, F. R. Gamble, and J. F. Revelli, Solid State Commun. **9**, 981 (1971).
- <sup>13</sup>J. F. Revelli, Jr., Ph.D. dissertation, Stanford University, 1973 (unpublished).
- <sup>14</sup>F. R. Gamble, J. H. Osiecki, M. Cais, R. Pisharody, F. J. Di Salvo, and T. H. Geballe, Science **174**, 493 (1971).
- <sup>15</sup>J. Cousseau, L. Trichet, and J. Rouxel, Bull. Soc. Chim. France **1973**, 872.
- <sup>16</sup>J. Bichon, M. Danot, and J. Rouxel, C. R. Acad. Sci. C (Paris) **276**, 1283 (1973).
- <sup>17</sup>A. L. Schawlow and G. E. Devlin, Phys. Rev. **113**, 120 (1959).
- <sup>18</sup>H. C. Montgomery, J. Appl. Phys. **42**, 2971 (1971).
- <sup>19</sup>R. Bachmann, F. J. Di Salvo, T. H. Geballe, R. L. Greene, R. E. Howard, C. N. King, H. C. Kirsch, K. N. Lee, R. E. Schwall, H-U. Thomas, and R. B. Zubeck, Rev. Sci. Instrum. **43**, 205 (1972).
- <sup>20</sup>R. E. Schwall, R. E. Howard, and G. R. Stewart, submitted to Rev. Sci. Instrum.
- <sup>21</sup>J. Edwards and R. F. Frindt, J. Phys. Chem. Solids **32**, 2217 (1971).
- <sup>22</sup>F. J. Di Salvo, R. E. Schwall, T. H. Geballe, F. R. Gamble, and J. H. Osiecki, Phys. Rev. Lett. **27**, 310 (1971).
- <sup>23</sup>R. E. Schwall, Ph.D. dissertation, Stanford University, 1973 (unpublished); R. E. Schwall, G. R. Stewart, and T. H. Geballe (to be published).
- <sup>24</sup>W. L. McMillan, Phys. Rev. **167**, 331 (1968).
- <sup>25</sup>J. A. Benda, C. N. King, K. R. Pisharody, and W. A. Phillips, in *Proceedings of Thirteenth International Conference on Low Temperature Physics*, Boulder, Colo., 1972, edited by R. H. Kropschot, W. J. O'Sullivan, and E. F. Hammel (Plenum, New York, 1974), Vol. 4, p. 423.
- <sup>26</sup>A. H. Thompson, Solid State Commun. **13**, 1911 (1973).
- <sup>27</sup>I. G. Austin and N. F. Mott, Adv. Phys. **18**, 41 (1969).
- <sup>28</sup>We are indebted to S. Doniach for this suggestion.
- <sup>29</sup>Charge density waves may also manifest themselves in other phenomena. We now believe that the temperature dependence of the magnetic susceptibility observed by Geballe *et al.* [T. H. Geballe, A. Menth, F. J. Di Salvo, and F. R. Gamble, Phys. Rev. Lett. **27**, 314 (1971)] below 30°K in intercalation complexes of 2H-TaS<sub>2</sub> and attributed by them to superconducting fluctuations could also be due to charge density waves. This latter possibility even seems more likely since more careful magnetic measurements made subsequently [Ref. 8] failed to establish the inverse temperature dependence of the magnitude of diamagnetic contribution.
- <sup>30</sup>P. G. deGennes, in *Superconductivity of Metals and Alloys* (Benjamin, New York, 1966), p. 260.
- <sup>31</sup>L. F. Mattheiss, Phys. Rev. Lett. **30**, 784 (1973); Phys. Rev. B **8**, 3719 (1973).
- <sup>32</sup>J. C. McMenamin and W. E. Spicer, Phys. Rev. Lett. **29**, 1501 (1972).
- <sup>33</sup>P. M. Williams and F. R. Sheperd, J. Phys. C **6**, 136 (1973).
- <sup>34</sup>J. V. Acrivos and J. R. Salem, Philos. Mag. **30**, 603 (1974).
- <sup>35</sup>A. H. Thompson, F. R. Gamble, and R. F. Koehler, Phys. Rev. B **5**, 2811 (1972).